Songklanakarin J. Sci. Technol.
32 (6), 613-618, Nov. - Dec. 2010

Songklanakarin Journal
of Science and Technology

http://www.sjst.psu.ac.th

Original Article

Study of the effect of solidification on graphite flakes microstructure and mechanical properties of an ASTM a-48 gray cast iron using steel molds

Ganwarich Pluphrach*

Department of Mechanical Engineering, Faculty of Engineering,
Srinakharinwirot University, Ongkharak, Nakhon Nayok, 26120 Thailand.

Received 1 July 2009; Accepted 31 December 2010

Abstract

The analysis of heat conduction is a widely used technique for control of metallurgical process and solidified eutectic alloy investigation. The objectives of this research are studies about the effect of solidification on graphite flakes microstructure and mechanical properties of an ASTM A-48 gray cast iron using SKD 11 tool steel, S45C medium carbon steel and SS400 hot-rolled steel molds. These three steel molds are important for heat conduction and different from other works. This analysis involving thermocouples immersed in the molten cast alloy is convenient to quickly obtain solidified ingot data on the behavior of solidification processing. This research intends to describe the thermal analysis using thermocouples, shape of thermal field and the experimental boundary conditions. The Newtonian thermal analysis and the Fourier thermal analysis differ because of the number of used thermocouples. Mechanical properties of structural ASTM A-48 gray cast iron materials strongly depend on their microstructure. Metallographic sections are observed to quantitatively measure the relevant microstructural parameters, as graphite lamellas morphology, eutectic cell size and inclusions content. Results are correlated to the measured mechanical properties: reduced graphite content increases the tensile strength.

Keywords: solidification, graphite flakes microstructure, mechanical properties, ASTM A-48 gray cast iron

1. Introduction

ASTM A-48 gray cast iron is one of the most important engineering materials. Machine tool beds, cylinder blocks, gears, piston ring, and many other parts are made of cast iron. The properties that make cast iron such an industrially valuable metal are its high castability, fair mechanical properties, excellent machinability, and its lack of sensitivity to the quality of surface finish. In the structure of gray cast iron, a large part or all of the carbon is in the form of flakes or nodules of graphite. Graphitic cast iron has a dark gray or almost black fracture (Xu *et al.*, 2005). Upon small degrees of supercooling, graphite is formed when the cast iron solidifies from its liquid state. Slow cooling promotes graphitization. Rapid cooling partly or completely suppresses graphitization and leads to the formation of cementite. When cast iron, in which the carbon is in the form of iron carbides, is heated to a high temperature and held for considerable time, graphitization will occur, i.e., the cementite will be transformed into graphite. In this process, inclusions of the stable phase of graphite nucleate and grow while cementite crystals dissolve. After a certain period of time, the metastable phase, cementite, disappears. The rate of graphitisation is limited by the slowest component process, which is self-diffusion of the iron, i.e., the process in which the iron atoms leave the places where graphite is formed. Various degrees of cementite decomposition may be obtained by changing the amount of graphite and carbide-forming elements in the cast iron. This is most easily accomplished in actual practice by varying the silicon content. In any given composition of cast iron, its structure will depend on the rate of cooling (wall thickness) of the casting. The structure obtained depending on the

* Corresponding author.
Email address: pganwarich@yahoo.com

composition (Si+C content) and the cooling rate (which practically may depend on the wall thickness of the casting). The relation between the properties of cast iron and its structure is much more complicated than that for steel. Gray cast iron consists of a metallic matrix in which graphite inclusions are disseminated. Therefore, the properties of cast irons will be determined by the structure of the matrix and the character of the graphite inclusions. The effect of the latter on the properties can only be qualitatively evaluated. The larger the inclusions and the less they are isolated, the weaker the cast iron will be with same matrix. The metallic matrix of common foundry cast iron consists of pearlite and ferrite. An increase in pearlite in the structure with the same form of graphite precipitation will improve the mechanical properties (Lakhtin, 1977).

1.1 Heat conduction on solidification

Cylindrical coordinates are the natural ones to use in this research because of the ease in specification of the boundary conditions. Of special interests are steady state conduction problems in such a cylindrical configuration but with the boundary conditions so chosen that axial symmetry exists. That is, if one considers problems in which there is no dependence on circumferential coordinate, the distribution of temperature in the cylinder depends only on the radial coordinate, r, and the axial coordinate, z. The conduction equation in cylindrical coordinates is as the following (Chapman, 1989):

$$\frac{\partial^2 \theta}{\partial r^2} + \frac{1}{r}\frac{\partial \theta}{\partial r} + \frac{\partial^2 \theta}{\partial z^2} = 0. \tag{1}$$

The solidification and structures of gray cast iron can be understood qualitatively in terms of the simple iron-carbon binary diagram, assuming complete diffusion of carbon in the austenite during and after solidification. In most casting and ingot-making processes, hot liquid is poured into a cold mold; specific heat and heat of fusion of the solidifying metal pass through a series of thermal resistance to the cold mold until solidification is complete. An essential element of all solidification processes is heat flow as a non-linear heat conduction problem expanded with a heat source corresponding to the released latent heat of solidification. The general case is written as (DiÓszegi and Svensson, 2004):

$$\rho C_p \frac{\partial T}{\partial t} = \nabla(k\nabla T) + \dot{q}_{sol} \tag{2}$$

where ρ is the density (kg m^{-3}), C_p the heat capacity (Jkg^{-1} K^{-1}), $\frac{\partial T}{\partial t}$ the cooling rate (°C s^{-1}), k the thermal conductivity (Wm^{-1}K^{-1}), T the temperature (°C) and $\dot{q}_{sol}$ is the released heat during solidification used in heat conduction equations (Wm^{-3}).

Thermal analysis based on the interpretation of a cooling curve from a single thermal point, also called the Newtonian Thermal Analysis. If k is assumed constant, Equation 2 can be expressed as (Diószegi and Svensson, 2004):

$$\frac{\partial T}{\partial t} = \alpha \nabla^2 T + \frac{\dot{q}_{sol}}{C_v} \; : \; \alpha = \frac{k}{\rho C_p} \text{ and } C_v = \rho C_p \tag{3}$$

where α is the thermal diffusivity (m^{2}s^{-1}), C_v the volumetric heat capacity (Jm^{-3}K^{-1}), and ∇^2T the Laplace operator.

1.2 Mechanical properties

Hardness and ultimate tensile strength are the most commonly specified properties for iron castings. Hardness is a relatively good indication of machinability, however, gray and ductile iron with the same hardness can exhibit appreciable differences in tool life. That is, if the microstructure of either contains some free carbides, machinability is reduced much more than indicated by the small increase in hardness. The mechanical properties of metal, especially iron, are not specific to a particular batch or heat as is the chemical analysis of metal. Properties are also influenced by the section thickness in which the metal solidifies and the manner in which the metal cools. The qualification results from the fact that the properties of iron are directly influenced by the rate of solidification and subsequent cooling. Appreciably different properties in various portions of a casting are apt to occur if the sections have sufficiently large differences in thickness or shape to cause a significant variation in cooling rate. With modern technology, however, castings can be more uniform throughout variously sized sections. Thus, both large and small casting from the same ladle of metal will have similar mechanical properties.

2. Experimental Procedure

A melt temperature of 1,350°C was applied for all the casting conditions. The thermal analysis methods has been applied to analyze cooling curves obtained from numerical simulation of three cylindrical domain presented in Figure 1. The material used in the simulation was an eutectic Fe–C alloy cast in steel molds. The simulation parameters are given in Table 2. The released latent heat defined according to Equation 3 the heat rate released in the solidification interval for the Newtonian zero line and Fourier thermal analysis method are mainly dependent on how the Newtonian and the Fourier zero line are determined. The calculated heat rate released in the solidification interval is expressed as a function of the fraction solid. The chemical composition (wt%) of materials at Table 1 in the simulation are an ASTM A-48 gray cast iron and three different cylindrical steel molds. The ASTM A-48 gray cast iron microstructure of some the relevant samples representative photomicrographs are taken. In order to determine the microstructure, the samples are

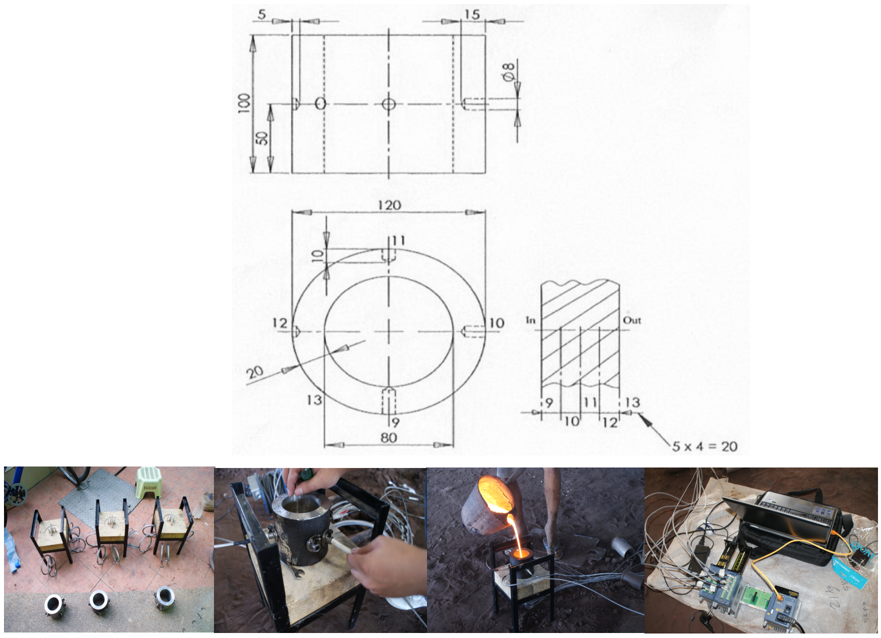

Figure 1. Solidified ASTM A-48 gray cast iron using three different steel molds as SKD 11 tool steel, S45C medium carbon steel and SS400 hot-rolled steel for analyzing simulated cooling curves from 13 different positions, the material solidified using thermocouple type K on PC-based data acquisition system as shown in details of the following. 1.1 The top three figures are shown working drawing of the steel molds, the right side is shown its sectional view on ninth to thirteenth position of the heat conduction testing using thermocouple type K. (These three figures are not to scale) 1.2 Left of the below four figures is shown three different steel molds and their supports. 1.3 Middle left of the below four figures is shown the connecting of thermocouples. 1.4 Middle right of the below four figures is shown the pouring of melting ASTM A-48 gray cast iron to a mold. 1.5 Right of the below four figures is shown the PC-based data acquisition system.

Table 1. Chemical composition (in wt%) of an ASTM A-48 gray cast iron and three different cylindrical steel molds.

Elements & Carbon equivalent	Gray cast iron	Mold 1SKD11 Tool steel	Mold 2S45C Medium carbon steel	Mold 3SS400 Hot-rolled steel
C	3.25	1.42	0.44	0.23
Si	1.52	0.33	0.20	0.23
Mn	0.75	0.34	0.62	0.43
P	0.15	0.022	0.012	0.012
S	0.1	0.007	0.005	0.005
Cr	0.15	11.44	0.05	0.01
Mo	0.006	-	-	-
Ni	0.029	0.15	0.04	0.4
Cu	0.07	0.05	0.05	0.04
Sn	0.11	-	-	-
Al	0.004	-	-	-
Mg	0.001	-	-	-
C.E.	3.807	-	-	-

specially etched in 3% nital solution (Pluphrach, 2005). The concentration of the nital solution has to be adjusted for different samples. The microstructure is then measured at magnification 100x using a filler eyepiece.

The α, α+Fe_3C or Fe_3C with graphite flakes microstructure determination should be done in a magnification suited to the size of the grain so that small grains may not be lost. The degree of magnification will be limited by the fact

Table 2. Thermal properties used in the solidification simulation of cylindrical steel molds.

Gray cast iron	Mold 1	Mold 2	Mold 3
T_{init} = 1,350°C	T_{init} = 30°C	T_{init} = 30°C	T_{init} = 30°C
T_{eq} = 1,150°C			
C_p = 0.42 kJkg^{-1}K^{-1}	C_p = 0.486 kJkg^{-1}K^{-1}	C_p = 0.465 kJkg^{-1}K^{-1}	C_p = 0.415 kJ kg^{-1}K^{-1}
ρ = 7,272 kg m^{-3}	ρ = 7,753 kg m^{-3}	ρ = 7,833 kg m^{-3}	ρ = 7,130 kg m^{-3}
k = 52 W m^{-1} K^{-1}	k = 36 W m^{-1} K^{-1}	k = 54 W m^{-1} K^{-1}	k = 54 W m^{-1} K^{-1}
L = 238 kJ kg^{-1}			
h = 1,050 Wm^{-2}K^{-1}	h = 1,250 Wm^{-2}K^{-1}	h = 1,200 Wm^{-2} K^{-1}	h = 1,200 Wm^{-2} K^{-1}

Note: T_{init} – temperature at which the start of simulation (°C), T_{eq} – temperature of equilibrium (°C), L – latent heat of solidification (kJ kg^{-1}), h – heat transfer coefficient (Wm^{-2} K^{-1}).

that the picture must include sufficient graphite flakes. For the mechanical properties, tensile and hardness samples are prepared from selected solidified ASTM A-48 gray cast iron and tested in tensile and hardness testing machine, respectively. Materials selection for mechanically loaded microcomponents is a challenging task. Even if the loads are small, the stresses may be very large. Tensile test micro-specimens made from ASTM A-48 gray cast iron with a composition indicated in Table 1 were fabricated by micro-casting based on the so-called casting method.

3. Result and Discussion

As-cast some important cast iron microstructure of the three steel molds are used to study the effect of solidification processes as shown in Figure 2. The ASTM A-48 material under examination is a lamellar gray cast iron with fully pearlitic matrix. Pearlite, characterized by high strength and hardness, is a product of eutectoid transformation and it is made up of alternate lamellar planes of ferrite and cementite. Ferrite, which has low strength and high ductility, is the Fe phase with low carbon content; its formation is favored by graphitizing elements, such as Si or by low cooling rates, characteristic of thick cast walls. Cementite is hard and brittle intermetallic.

The formation of Fe–C compound is favored in zones of castings characterized by high cooling rates, such as thin-wall sections, corners, or at the external surfaces. Properties of pearlite strongly depend on spacing between ferrite–cementite planes: the mechanical strength of pearlite increases when the interlamellar spacing decreases, for example by fast cooling (Budinski and Budinski, 2007). The chemical compositions of ASTM A-48 gray cast iron used for steel molds 1-3 are reported in Table 1. They slightly differ from each other in C, Si, Mn, P, S, and Cr–content, but all elemental contents are within the range prescribed by the standard. The carbon equivalent content for this research material is 3.807% (Mills *et al.*, 1985). A typical pearlitic microstructure of gray cast iron is shown in the micrograph of Figure 3.

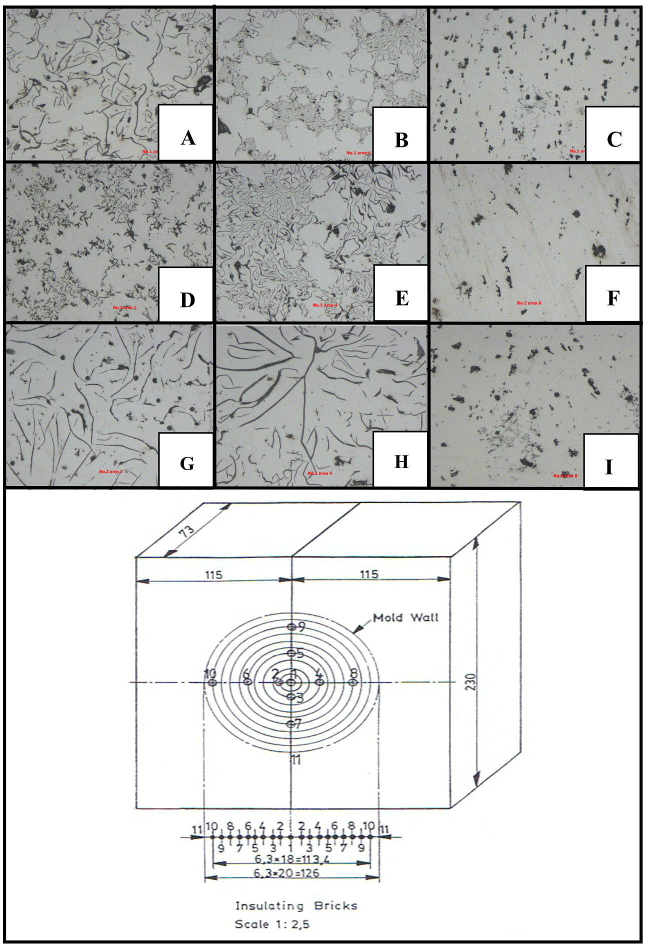

Figure 2. Microstructure of solidified gray cast iron from the three steel molds [Mold SKD 11 at picture A,B,C, Mold S45C at picture D,E,F, and Mold SS400 at picture G,H,I, those from position 1 (picture A of Mold SKD 11, picture D of Mold S45C, picture G of Mold SS400), position 4 (picture B of Mold SKD 11, picture E of Mold S45C, picture H of Mold SS400) and position 8 (picture C of Mold SKD 11, picture F of Mold S45C, picture I of Mold SS400) in the axial direction model of heat conduction as shown in working drawing] on the same magnification as 50 µm ▬.

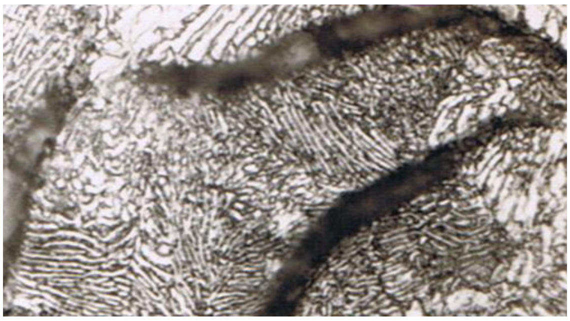

Figure 3. Metallographic section of pearlitic microstructure of gray cast iron showing graphite flakes in the matrix of alternate planes of ferrite and cementite, etched with Nital 3%, on the magnification as 20 µm .

The time versus temperature helps to visualize the temperature contours and distribution inside the solidifying ASTM A-48 gray cast iron form simulation. So, the effect of the particle hindrance by the solid–liquid interface can be thoroughly studied. The extended thermocouple wires from the mold are connected to the input terminals of the data acquisition system and the corresponding output leads are linked to the computer. By using a suitable graphic package, the used computer software helps to generate the time-temperature data readings. Simulated cooling curves show from different positions in the cylindrical domain, which have been used for thermal analysis. The released latent heat defined according to Equation 3 for the Newtonian Thermal Analysis method that rearranging a substituting $\dot{q}_{sol}$ by q_s, and the Fourier Thermal Analysis method are mainly determined. According to the NTA the solidification rate attain a maximum in the first half of the solidification interval and decrease continuously afterwards until the end of solidification. Due to the known solidification rates in every node of the simulated cylindrical domain, it is possible to analyze the validity of the different thermal analysis methods by comparing the simulated solidification rates to the calculated solidification rates. The ASTM A-48 gray cast iron with ferrite-cementite matrix and graphite flakes are embedded as shown in picture A and B of the Figure 2 and in Figure 3. Ultimate tensile strength and Brinell hardness number of every pictures of solidified gray cast iron microstructure in Figure 2 are shown in Table 3. Ultimate tensile strength and Brinell hardness number of picture A are lower than picture B. This is because in the same tool steel mold SKD 11, the position 4 as picture B has smaller graphite flakes than the position 1 as picture A and is called 'mottled structure'. The microstructure of picture C consists of pearlite-cementite and ledeburite, it is called white cast iron, because it shows a white fractured surface. A squeeze casting process model is analyzed for data of generating time-temperature, microstructure and mechanical properties during the process of solidification. As in squeeze casting process, the pressure and heat conduction are applied until the casting gets solidified completely in the steel molds (Pluphrach, 2005; 2008). For this reason, the influence of heat conduction on mechanical properties and microstructural development of the three steel molds can be shown by the pictures and data given in Table 3 and Figure 2.

The microstructure of ASTM A-48 gray cast iron usually consists of graphite flakes and a matrix of pearlite and/or ferrite; its mechanical properties mainly influence the machining performance. The base experimental alloy given in Table 1 is found to have an UTS and BHN, despite this alloy also exhibiting the ferrite-cementite with graphite flakes embedded, mottled and pearlite-cementite/ledeburite microstructure after solidified in the three solid steel molds. The improvement in mechanical properties is probably the result of the addition of 0.07 wt% Cu, which is known to be a reasonable solid solution strengthener of ferrite and also acts to refine the pearlite spacing. The alloying additions Mo, Mn, Si, and Cu during steel mold casting of this research material of base composition (wt%) Fe–3.25C–0.75 Mn–1.52 Si are found to generate a wide range of microstructure and mechanical properties. Regardless of the amount and type of alloying addition, type E graphite forms in all alloys. For

Table 3. Ultimate tensile strength and Brinell hardness number for every sample according to the pictures of solidified gray cast iron microstructures in Figure 2.

Picture	Ultimate tensile strength (MPa)	Brinell hardness number (BHN)
A	280	290
B	312	320
C	330	340
D	308	319
E	315	325
F	338	342
G	290	309
H	292	289
I	343	345

Mo-free gray iron, various combinations of Mn, Cu and Si do not promote the formation of a microstructure containing an intimate dispersion of austenite and bainitic ferrite, but a pearlitic alloy containing graphite flakes is produced.

4. Conclusions

Casting solidification simulation process is used to identify the defective locations in the castings from the generated time-temperature contours. It is used to determine the cooling rate influenced by the grain structure of castings. The time-temperature plot explains the effect of under cooling of solidifying castings which reflects more on the inside microstructure responsible for material properties. Thermal analysis of solidification is a technological complex procedure. The measured cooling curves collected from simple shape castings test cylinders have to be treated carefully. The number of thermocouples introduced in eight thermal fields of a solidifying cast alloy has significance on the quality of the interpreted results. A solidification simulation of the test cylinder has been done by a simulation code including kinetic models for calculation of the release of latent heat. The simulation parameters are given in Table 2. The calculated solidification time-temperature is plotted in Figure 4, 5 and 6.

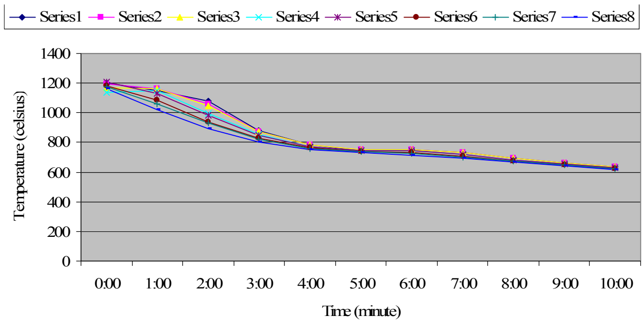

Figure 4. Time-temperature curve generated from the computer solidification simulation of an ASTM A-48 gray cast iron in the mold SKD 11, for position 1 to 8.

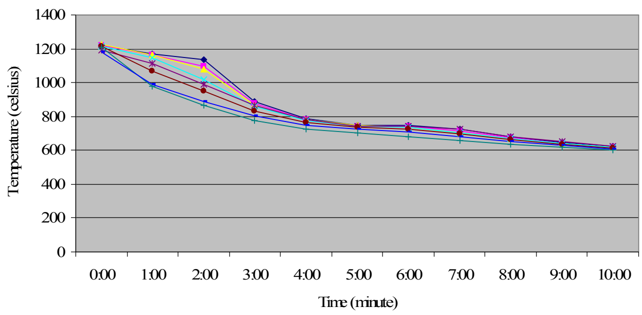

Figure 5. Time-temperature curve generated from the computer solidification simulation of an ASTM A-48 gray cast iron in the mold S45C, for position 1 to 8.

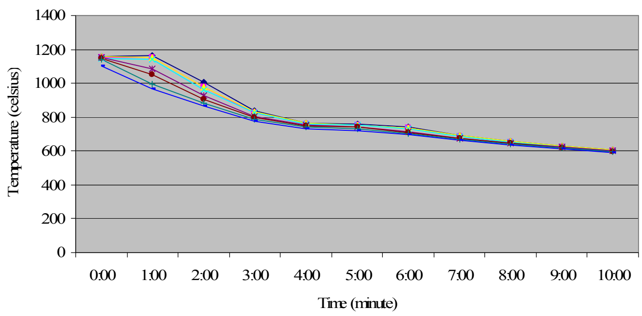

Figure 6. Time-temperature curve generated from the computer solidification simulation of an ASTM A-48 gray cast iron in the mold SS400, for position 1 to 8.

Acknowledgements

The author express his sincere gratitude to the Department of Mechanical Engineering and Faculty of Engineering, Srinakharinwirot University, Thailand, for a helpful discussion, and the SWU Research Department for the financial support of performing this research work under the Project agreement 036/2551 is acknowledged and for the consent to publish this paper.

References

Budinski, K.G. and Budiski, M.K. 2007. Engineering Materials Properties and Selection, 8th ed., Prentice-Hall of India private limited, New Delhi, India. pp. 593-612.

Chapman, A.J. 1989. Heat Transfer, 4th ed., Maxwell Macmillan international edition. New York, U.S.A., pp. 94-95.

Diószegi, A. and Svensson, I.L. 2004. A comparison of Fourier vs. Newtonian thermal analyse and its influence on the inverse kinetic growth calculation, Dissertation No.871, Linköping studies in Science and Technology, Supplement VI, pp. 311-318.

Lakhtin, Y. 1977. Engineering Physical Metallurgy 6th ed., Mir Publishers, Moscow, the Union of Soviet Socialist Republics, pp. 369-377.

Mills, K. *et al.*, 1985. Metals Handbook, vol. 9, ASM International, pp.320-325.

Pluphrach, G. 2005. Effect of Vanadium Additions on Yield Stress of Low Carbon Microalloyed Cast Steels. Srinakharinwirot Science Journal 19-21, 102-107.

Pluphrach, G. 2008. Mechanical Propeties and Microstructure of Plain Low-Carbon Steels after Quenching, Research and Development Journal of the Engineering Institute of Thailand Under H.M. The King's Patronage, 10(2), 65-71.

Pluphrach, G. 2009. Mechanical Engineering Research Methodology, Top Publishing Co., Ltd., Bangkok, Thailand, pp. 131-203.

Xu, W., Ferry, M. and Wang, Y. 2005. Influence of alloying elements on as-cast microstructure and strength of gray iron, Materials Science and Engineering A 390 pp. 326-333.